Integrated-optical polarization mode dispersion compensation for 6-ps, 40-Gb/s pulses

D. Sandel, S. Hinz, M. Yoshida-Dierolf, V. Mirvoda, R. Noé (1),

G. Feise, H. Herrmann, R. Ricken, W. Sohler, H. Suche, F. Wehrmann, R. Wessel (2)

(1) Optical Communications and High-Frequency Engineering (noe@uni-paderborn.de);

(2) Applied Physics; (1) and (2): University of Paderborn, Warburger Str. 100, 33098 Paderborn, Germany

Abstract: *PMD compensation on RZ signals is demonstrated for the first time, using a distributed Ti:LiNbO3 PMD compensator. An electrical PMD detection scheme maintains the pulse width at <6 ps.*

Introduction: Polarization mode dispersion (PMD), especially in installed fiber, broadens optical pulses in a time-variant manner and therefore impedes the development of highest-capacity, long-haul communication systems.

At the receive end PMD has been optically compensated by equalizers with one or a few differential group delay (DGD) sections and polarization transformers /1–5/ and by distributed equalizers with polarization transformers embedded in a birefringent waveguide /6-8/, but only for NRZ signals. For RZ signals PMD-induced penalties have been investigated /9/. Here we assess the compensation capability of a distributed LiNbO3 PMD compensator /8/ for 6-ps RZ pulses at 40 Gb/s data rate.
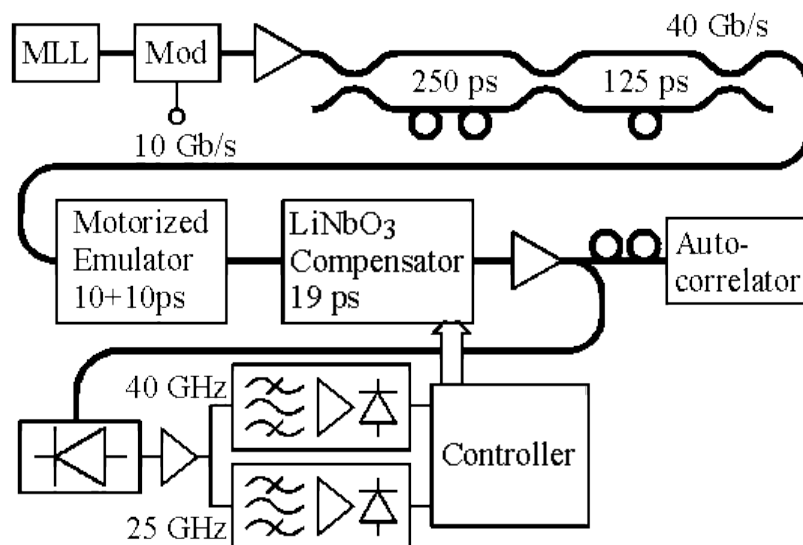

Fig. 1: Experimental setup

Setup: A 10 GHz modelocked Ti:Er:LiNbO3 waveguide laser (MLL) /10, 11/ was used as an optical source (Fig. 1). It emitted a stable train of 5.9 ps (FWHM) pulses at λ = 1561 nm with a time-bandwidth product of 0.56. It was externally modulated at 10 Gb/s.

With two delay lines and couplers the signal was optically multiplexed to a data rate of 40 Gb/s. A PMD emulator with two pieces of polarization-maintaining fiber (PMF), preceded, separated and followed by a total of 8 motorized fiber loop devices, simulated a transmission fiber. PMD was compensated in a distributed X-cut, Y-propagation LiNbO3 PMD compensator with ~ 0.26 ps/mm of DGD caused by material and waveguide birefringence. The device was 70 mm long and carried 50 sections in which mode conversion in phase and in quadrature was possible by means of voltages applied to appropriately placed comb electrodes. 100 voltages of $\pm\leq$ 69 V were applied. Insertion loss was 4.4 dB, with a $\pm$0.3 dB variation depending on polarization (when zero voltages were applied). Pigtailed chip and voltage sources

form a compact unit /8/. The total compensatory power was 19 ps of DGD.

At the receive end the signal was detected in a 40 GHz photodiode (u2t Innovative Optoelectronic Components). The electrical signal was amplified and then analyzed in two spectral power meters. One of them was a spectrum analyzer tuned to the 40 GHz clock line, and the other contained band-limited amplifiers having a 25 GHz center frequency and a 10 GHz bandwidth. Fig. 2 shows that very sensitive PMD detection is possible. The signals were read into a PC which worked as a controller. A SHG autocorrelator was used to monitor the received pulse width.
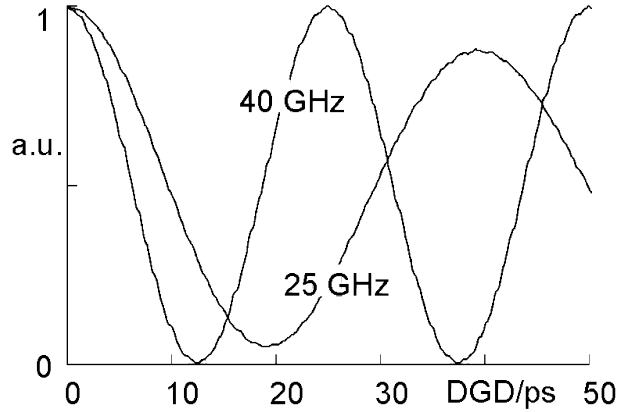
Fig. 2: Calculated powers at 25 and 40 GHz as a function of 1st-order PMD

Experiment: The optical autocorrelator is polarization-dependent and slow, and for this reason it can only measure at static PMD. The following measurements were therefore repeated several times, and polarization was always adjusted for highest sidelobes or pedestals due to PMD.

Fig. 3a shows the back-to-back autocorrelation trace. Only the center and one half are shown because the other (mirrored) half is not accessible due to a limited scanning range. At delay multiples of the 25 ps bit period the autocorrelation signal exhibits peaks. Due to the PRBS modulation these are half as high as the peak at zero delay. The FWHM is 8.3 ps, and this corresponds to a deconvolved 5.9 ps pulse width.

As a next step the PMD compensator was inserted. The controller maximized the 25 and 40 GHz power levels. The autocorrelation trace reveals a slightly narrower pulse with a deconvolved 5.2 ps width (Fig. 3b). Similar pulse peaking has already been found in NRZ experiments /3, 6, 8/. Then the emulator was inserted with 10 + 6 ps of DGD in the PMF pieces. The deconvolved pulse width was now 5.4 ps but the autocorrelation pedestal (3% back-to-back) increased to 7.5% (Fig. 3c). With 10 + 10 ps of DGD in the emulator the deconvolved pulse width was 5.8 ps and the pedestal 12% (Fig. 3d). However, the autocorrelation function exaggerates the true pedestal, as may be seen from a deconvolution result assuming the superposition of two Gaussian pulses (Fig. 3e). There is very little intersymbol interference. For comparison we give also an autocorrelation trace for emulator plus compensator with the control signals minimized rather than maximized. In this case the original pulses essentially disappear due to PMD (Fig. 3f).
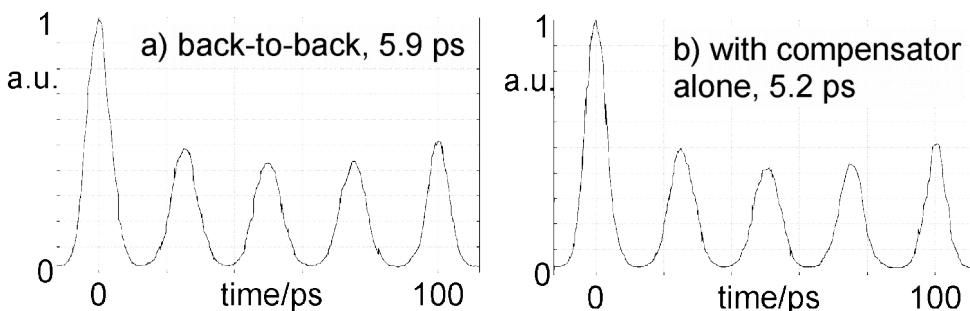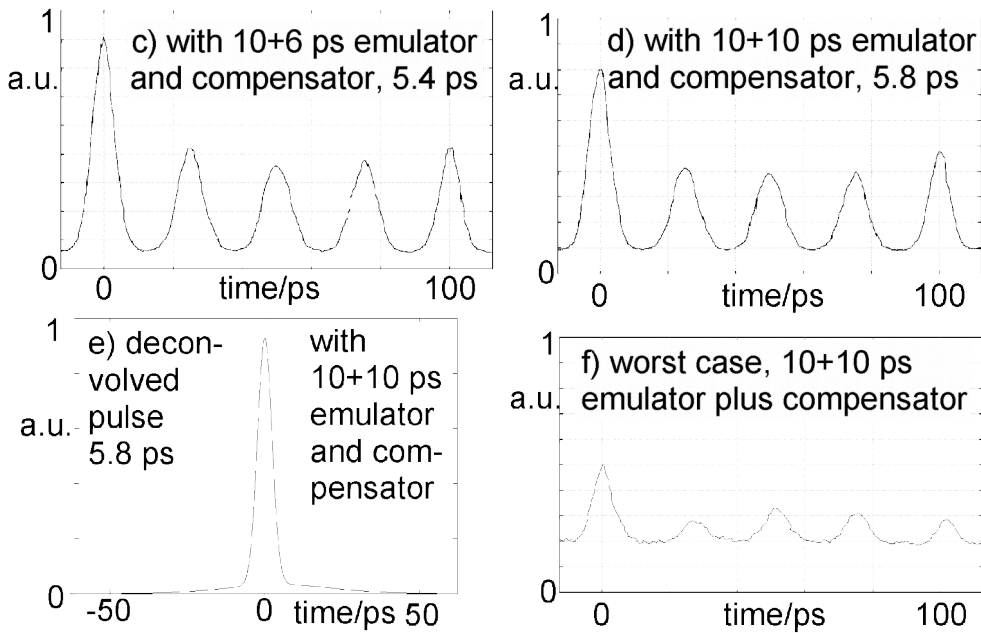
Fig. 3: Autocorrelation traces

A dynamic measurement was made with the 10 + 6 ps emulator and the compensator. Starting from an initial standstill the motorized fiber polarization transformers were made to turn successively faster.
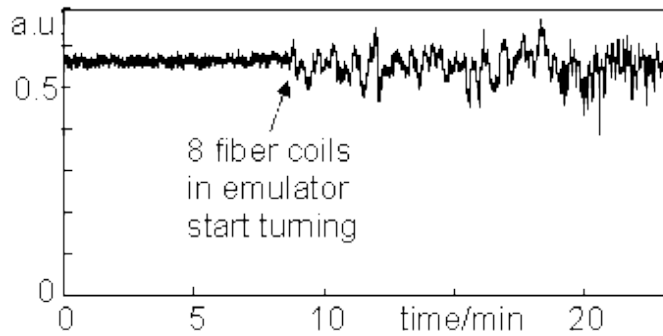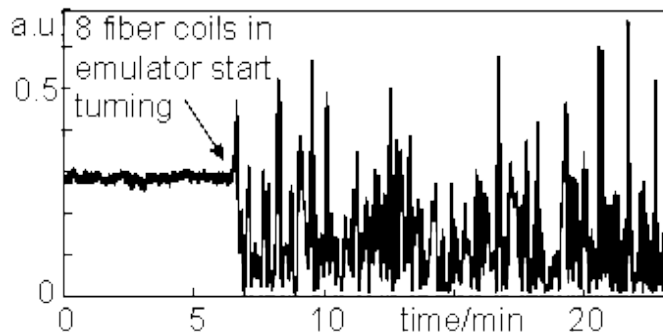

Fig. 4: Spectral power recorded during control

Fig. 5: Spectral power recorded while control is off

Fig. 4 shows an aggregate control signal obtained by linearly combining the 40 and 25 GHz power level signals. Part of the signal variations can be attributed to polarization dependence (~ 1 dB) of the components following the compensator. For a comparison the measurement was repeated when control was off. Large signal fluctuations occurred as expected when the fiber coils started to turn (Fig. 5).

The experiment shows that optical PMD compensation with a simple, purely electrical PMD detection scheme is possible also for RZ signals.

Conclusions: PMD of RZ signals has been compensated, for the first time to our knowledge. A distributed LiNbO3 PMD compensator was used to equalize 6-ps, 40 Gb/s pulses distorted by 10 + 10 ps of DGD, using a 10 GHz modelocked Ti:Er:LiNbO3 waveguide laser.

References:

1. T. Takahashi, T. Imai, M. Aiki, Electron. Lett. 30 (1994) 4, pp. 348-349

2. F. Heismann, D.A. Fishman, D.L. Wilson, ECOC '98, Madrid, Spain, WdC11

3. D. Sandel et al., Electronics Letters 34(1998)23, pp. 2258–2259.

4. M.W. Chbat et al., OFC/IOOC '99, PD12, San Diego, 21-26 Feb. 1999.

5. H. Ooi, Y. Akiyama, G. Ishikawa, OFC/IOOC '99, WE5, San Diego, 21-26 Feb. 1999.

6. R. Noé et al., Electronics Letters 34(1998)25, pp. 2421-2422.

7. David Sandel, Reinhold Noé, Proc. 9th European Conference on Integrated Optics (ECIO'99), April 14-16, 1999, Turin, Italy, ThB4

8. C. Glingener et al., OFC/IOOC '99, PD29, San Diego, 21-26 Feb. 1999.

9. R. M. Jopson et al., OFC/IOOC '99, WE3, San Diego, 21-26 Feb. 1999.

10. R. Wessel et al., Proc. 9th European Conference on Integrated Optics (ECIO'99), April 14-16, 1999, Turin, Italy, ThE1

11. H. Suche et al., IEEE J. of Quantum Electr., 33, (9), pp. 1642-1646, (1997)